Journal of Food and Drug Analysis

Volume 31 | Issue 3 Article 10

# Autophagy-urea cycle pathway is essential for the statin-mediated nitric oxide bioavailability in endothelial cells

ORIGINAL ARTICLE

# Autophagy—urea cycle pathway is essential for the statin-mediated nitric oxide bioavailability in endothelial cells

Wen-Hua Chen [a], Bei-Chia Guo [a], Chia-Hui Chen [a], Man-Chen Hsu [a], Chih-Hsien Wang [b,**], Tzong-Shyuan Lee [a,*]

[a] Graduate Institute and Department of Physiology, College of Medicine, National Taiwan University, Taipei, Taiwan
[b] Cardiovascular Surgery, Department of Surgery, National Taiwan University Hospital and College of Medicine, Taipei, Taiwan

## Abstract

**Statins induce nitric oxide (NO) bioavailability by activating endothelial nitric oxide synthase via kinase- and calcium-dependent pathways in endothelial cells (ECs). However, their effect on the metabolism of L-arginine, the precursor for NO biosynthesis, and regulatory mechanism have not yet been investigated. In this study, we investigated the role of the autophagy—urea cycle-L-arginine pathway in simvastatin-mediated NO bioavailability in ECs. Griess's assay was used to determine the NO bioavailability. Protein expression was assessed using Western blot analysis. Further, immunocytochemistry was performed to observe autophagosome formation, while conventional assay kits were used to quantify the levels of different intermediate substrates of the urea cycle. In ECs, treatment with simvastatin induced the activation of autophagy flux, as evidenced by the increased levels of microtubule-associated protein 1A/1B-light chain 3 II and autophagolysosome formation and decreased levels of p62. Inhibition of autophagy by ATG7 small interfering RNA (siRNA), chloroquine and bafilomycin A1 abolished simvastatin-induced NO bioavailability, EC proliferation, migration, and tube formation. Additionally, simvastatin increased the intermediate substrates levels of the urea cycle, including glutamate, acetyl-CoA, urea, and L-arginine, all of which were abrogated by chloroquine or bafilomycin A1. Genetic knockdown of argininosuccinate lyase using siRNA abrogated simvastatin-induced increase in NO bioavailability and EC-related functions. Moreover, inhibition of AMP-activated protein kinase (AMPK) and transient receptor potential vanilloid 1 (TRPV1) prevented simvastatin-induced activation of the autophagy—urea cycle pathway and NO production. Our findings suggest that simvastatin activates the autophagy—urea cycle pathway via TRPV1-AMPK signaling, which increases L-arginine bioavailability and ultimately promotes NO production in ECs.**

*Keywords:* Autophagy, Nitric oxide, Statin, Urea cycle

## 1. Introduction

Statins, inhibitors of 3-hydroxy-3-methylglutaryl coenzyme A (HMG-CoA) reductase, are widely used to treat hypercholesterolemia and reduce the risk of cardiovascular events [1]. Mechanistically, statins promote low-density lipoprotein (LDL) clearance by upregulating LDL receptor (LDLR)

*Abbreviations:* AMPK, AMP-activated protein kinase; ASL, argininosuccinate lyase; ATG7, autophagy related 7; BafA1, bafilomycin A1; $Ca^{2+}$, calcium; C.C., compound C; CPZ, capsazepine; CQ, chloroquine; CAT-1, cation amino acid transporter 1; EC, endothelial cell; eNOS, endothelial nitric oxide synthase; HMECs, human microvascular ECs; LC3, microtubule-associated protein 1A/1B-light chanis 3; LDL, low-density lipoprotein; LDLR, low-density lipoprotein receptor; NO, nitric oxide; PKA, protein kinase A; PKC, protein kinase C; siRNA, small interfering RNA; SREBP2, sterol regulatory element-binding protein 2; TRPV1, transient receptor potential vanilloid 1; T2D, type 2 diabetes.

Received 30 November 2022; accepted 11 July 2023.
Available online 31 August 2023

* Corresponding author at: Graduate Institute and Department of Physiology, College of Medicine, National Taiwan University, Taipei 10051, Taiwan.
** Corresponding author at: Cardiovascular Surgery, Department of Surgery, National Taiwan University Hospital and College of Medicine, Taipei 10051, Taiwan.
E-mail addresses: wchemail@ntu.edu.tw (C.-H. Wang), ntutslee@ntu.edu.tw (T.-S. Lee).

https://doi.org/10.38212/2224-6614.3472

expression in the liver, leading to a decrease in circulating levels of LDL [2]. In addition to the cholesterol-lowering effect, statins have pleiotropic effects on the physiological functions of endothelial cells (ECs) to improve endothelial function by increasing nitric oxide (NO) bioavailability and protecting against cardiovascular diseases [3–6]. We and others have previously reported that simvastatin-induced NO production is due to the activation of endothelial nitric oxide synthase (eNOS) through transient receptor potential vanilloid receptor 1 (TRPV1)/calcium ($Ca^{2+}$)- and AMP-activated protein kinase (AMPK)-dependent signaling pathways [7–11]. Subsequently, activated eNOS catalyzes the conversion of L-arginine to NO and the co-product L-citrulline [11–13]. Additionally, endogenous *de novo* L-arginine production is tightly regulated by the enzymes involved in urea cycle such as argininosuccinate lyase (ASL) [14]. Although the mechanisms by which simvastatin regulates eNOS activity have been well-established [7–13], the effect of simvastatin on L-arginine metabolism and its molecular regulation remain elusive.

Autophagy is a conserved self-eating process that is important for cellular homeostasis; the macromolecules are degraded and cellular components are recycled, particularly to maintain the energy balance and amino acid pools under pathophysiological conditions [15–18]. The autophagy pathway is a complex process that starts with the formation of the phagophore and ends with the death of the autophagosome [19]. Several key kinases and regulators, including mammalian target of rapamycin complex 1, autophagy-related proteins, AMPK, beclin-1, microtubule-associated protein 1A/1B-light chain 3 (LC3), and p62, are known to be involved in this conserved process [19,21]. Upon amino acid deprivation or glucose starvation, AMPK triggers the activation of autophagy flux to generate amino acids for new protein synthesis and to maintain glucose homeostasis for cell survival [20–23]. Hence, autophagy is a crucial process for regulating cell survival and physiological functions of the cardiovascular system, while defective autophagy accelerates the progression of cardiovascular diseases [24,25]. For instance, deficiency in endothelial autophagy leads to endothelial dysfunction and promotes atherosclerosis [26,27], while activation of autophagy restores impaired eNOS activation and enhances NO production under high-glucose conditions [28]. Moreover, several lines of evidence suggest that autophagy is required for shear stress-induced NO production, which prevents ECs from inflammation and confers an atheroprotective effect [28–30]. However, the role of autophagy and the molecular mechanisms underlying the beneficial effects of simvastatin on NO production and EC function remain to be elucidated.

Given the beneficial effects of statins on the vascular system, in this study, we aimed to investigate the role of the autophagy–urea cycle-L-arginine pathway in simvastatin-upregulated NO bioavailability in ECs. We first investigated the role of autophagy in simvastatin-induced NO production and its proangiogenic effects. Second, we examined the effect of simvastatin on activation of the urea cycle-L-arginine pathway. Third, we defined the interplay between TRPV1-AMPK signaling and the autophagy–urea cycle-L-arginine pathway in simvastatin-induced NO bioavailability. We show that simvastatin triggers TRPV1-AMPK signaling and activates the autophagy–urea cycle pathway, which leads to eNOS activation and L-arginine bioavailability, promoting NO production. Therefore, our results suggest that the autophagy–urea cycle-L-arginine pathway plays a crucial role in regulating simvastatin-mediated NO production in ECs.

## 2. Materials and methods

### 2.1. Reagents

Simvastatin, lovastatin, rosuvastatin, atorvastatin, acridine orange, bafilomycin A1 (BafA1), chloroquine (CQ), and Compound C (C.C.) were purchased from Cayman Chemicals (Ann Arbor, MI, USA). 3-(4,5-Dimethylthiazol-2-yl)-2,5-diphenyltetrazolium bromide (MTT) assay kit, Griess reagent, capsazepine (CPZ), and SB-366791 were purchased from Sigma–Aldrich (St. Louis, MO, USA). LY294002 was obtained from Calbiochem (San Diego, CA, USA). Matrigel was purchased from Corning, Inc. (Corning, NY, USA). Rabbit antibodies for LC3 (#4108) and p62 (#5114) were purchased from Cell Signaling Technology (Beverly, MA, USA). Rabbit antibodies against AMPK (A12718) and cation amino acid transporter 1 (CAT1, A14784) were purchased from ABclonal Science (Woburn, MA, USA). Rabbit antibodies for autophagy related 7 (ATG7, ab133528) and LDLR (ab52818) were from Abcam (Cambridge, MA, UK). Mouse antibody for α-tubulin was purchased from Croyez (Taipei, Taiwan). Mouse antibody against ASL (sc-166787), ATG7 siRNA (siATG7, sc-41447), AMPK siRNA (siAMPK, sc-45312), and ASL siRNA (siASL, sc-61998) were purchased from Santa Cruz Biotechnology (Santa Cruz, CA, USA). Lipofectamine RNAiMAX transfection reagent was purchased from

Thermo Fisher Scientific (Waltham, MA, USA). Mouse antibody against sterol regulatory element-binding protein 2 (SREBP2, 557037) was from BD Bioscience (San Jose, CA, USA). Colorimetric/fluorometric kits for acetyl-CoA (#K317-100), urea (#K375-100), arginine (K384-100), glutamate (#K629-100), and ornithine (#K939-100) were purchased from BioVision (Milpitas, CA, USA).

### 2.2. Cell culture

Human microvascular ECs (HMECs) were obtained from the Centers for Disease Control (Atlanta, GA, USA). HMECs were cultured in Dulbecco's modified Eagle's medium (DMEM) supplemented with 5% fetal bovine serum (FBS), 100 U/mL penicillin, 100 μg/mL streptomycin, and 20% EC Growth Medium MV2 (Promocell, Heidelberg, Germany) containing 5% fetal calf serum, 5 ng/mL epidermal growth factor, 10 ng/mL basic fibroblast growth factor, 20 ng/mL insulin-like growth factor, 0.5 ng/mL vascular endothelial growth factor 165, 1 μg/mL ascorbic acid, and 0.2 μg/mL hydrocortisone.

### 2.3. Western blot analysis

Cells were lysed in immunoprecipitation lysis buffer, which contained 50 mM Tris–HCl pH 7.5, 5 mM EDTA, 300 mM NaCl, 1% Triton X-100, 1 mM phenylmethylsulfonyl fluoride, 10 μg/mL leupeptin, and 10 μg/mL aprotinin. Aliquots of lysates were separated by sodium dodecyl sulfate-polyacrylamide gel electrophoresis (SDS-PAGE) and transferred onto a polyvinylidene fluoride membrane (Millipore, Bedford, MA, USA). After being blocked with 5% skim milk for 1 h at 25 °C, the blotting membrane was incubated with primary antibodies overnight and then with corresponding secondary antibody for 2 h. Protein bands were visualized using an enzyme-linked chemiluminescence detection kit (PerkinElmer, Boston, MA, USA) and quantified using TotalLab 1D (Newcastle Upon Tyne, UK).

### 2.4. Visualization of acidic vesicular organelles

Living cells were stained with acridine orange (2.7 μM) in the culture medium for 15 min at 37 °C to visualize intracellular acidic vacuoles, including lysosomes, endosomes, and autophagosomes. The fluorescence of acridine orange staining was analyzed at the excitation/emission spectra of 502/525 nm, 460/650 nm, and 475/590 nm and was measured using SpectraMax i3x fluorometry (San Jose, CA, USA). The ratio of red to green fluoresce indicated the levels of acidic vesicular organelles and represents the levels of autolysosome formation. Images were captured under a Nikon TE2000-U microscope with an image analysis system.

### 2.5. Immunocytochemistry

HMECs were seeded into 4-well plate and incubated with the test reagents for 9 h, and fixed with 4% paraformaldehyde for 15 min. After permeabilization with 70% alcohol for 30 min at 25 °C, cells were blocked with 2% bovine serum albumin (BSA) for 1 h at 25 °C. Cells were incubated with the rabbit anti-LC3 antibody for 2 h at 25 °C and subsequently with the corresponding secondary antibody overnight at 4 °C. The number of LC3-II puncta was counted under photomicrographs which were digitally captured using a Leica DMIRB microscope equipped with LAS V4.12 software.

### 2.6. Measurement of urea cycle intermediates

The levels of urea cycle intermediates, including acetyl-CoA, glutamate, arginine, ornithine, and urea in HMECs were measured using assay kits, according to the manufacturer's instructions. The fluorescence of acetyl-CoA, arginine, and ornithine was analyzed at the excitation/emission spectra of 535/587 nm and was measured by SpectraMax i3x fluorometry. The amount of glutamate and urea was quantified by microplate spectrophotometer (Thermo Fisher Scientific, Waltham, MA, USA) at 450 nm. The value of Δ represents the concentration difference from each group and the group of 0 h or vehicle group.

### 2.7. Small interfering RNA transfection

HMECs were seeded in 3.5 cm dishes and then starved for 6 h in DMEM with 0.5% FBS and 2% EC Growth Medium MV2. After starvation, scramble siRNA, ASL siRNA, AMPK siRNA, or ATG7 siRNA mixed with Lipofectamine RNAiMAX transfection reagent was added to DMEM with 0.5% FBS and 2% EC Growth Medium MV2 and incubated for 24 h. The medium was replaced with fresh and normal DMEM and transfected cells were subjected to further experiments.

### 2.8. Determination of nitrite production

NO is metabolized to nitrites and nitrates. Hence, the nitrite levels were determined by mixing cell culture medium with an equal volume of Griess

reagent and incubating for 15 min at 25 °C. The absorbance of the samples was determined at 540 nm using a microplate spectrophotometer. Sodium nitrite was used as a standard to calculate the level of nitrite in culture medium, which was normalized relative to the cellular protein concentration.

### 2.9. Cell proliferation assay

HMECs were cultured in 12-well plates in serum-free medium for starvation for 12 h. After treatment, the cells were incubated with the MTT reagent for 3 h. The absorbance of the samples was measured at 570 nm wavelength using a microplate spectrophotometer.

### 2.10. Cell migration assay

The transwell migration assay was performed using modified chambers inserted into 24-well plates. HMECs were added to the upper chamber with serum free medium, and 5% FBS medium was added to the lower chamber. After the indicated treatment, the chamber was fixed with 4% paraformaldehyde for 10 min, and unmigrated cells on the upper side of the membrane were removed, while the migrated cells on the lower side of the membrane were stained with crystal violet. The number of migrating cells on the lower side of the membrane was counted in three randomly selected areas, which were captured using a Nikon TE2000-U microscope equipped with an image analysis system (QCapture Pro 6.0, QImaging, Surrey, BC, Canada).

### 2.11. Wound healing assay

HMECs were seeded onto 3.5 cm dishes in serum-free medium for starvation. A linear wound was made by scratching the bottom of the dish using a sterile 1 mL pipette tip. After scratching, the cells were washed with PBS and incubated in serum-free medium in indicated treatments for 18 h. The number of migrating cells between the dotted lines was quantified in three areas chosen randomly and compared with vehicle-treated group, and images were captured using a Nikon TE2000-U microscope with an image analysis system.

### 2.12. Tube formation

Matrigel was coated onto 3.5 cm dishes and polymerized for 2 h at 37 °C. HMECs were seeded onto the Matrigel layer and incubated with the indicated treatments for 12 h. The number of circles surround by HMECs, which is defined as tube formation, was calculated in three areas chosen randomly, and images were captured using a Nikon TE2000-U microscope equipped with an image analysis system.

### 2.13. Statistical analysis

The results are presented as mean ± standard error of the mean (SEM) calculated from five independent experiments. The Mann–Whitney U test was used to compare data between the two groups. One-way analysis of variance (ANOVA) followed by Fisher's Least Significant Difference was used to compare data of more than two groups. SPSS software v8.0 (SPSS Inc., Chicago, IL, USA) was used for all statistical analyses. Differences were considered statistically significant at $P < 0.05$.

## 3. Results

### 3.1. Simvastatin promotes NO bioavailability by activating autophagy

To determine whether simvastatin activated autophagy in ECs, HMECs were treated with simvastatin (1 μM) for the indicated time period. Western blot analysis showed that compared with the vehicle-treated group, treatment with simvastatin increased the protein level of LC3-II and decreased the protein level of p62 in a time-dependent manner (Fig. 1A–C) and concentration-dependent manner (Fig. S1). The exposure of HMECs to various statins including simvastatin, rosuvastatin (1 μM), lovastatin (1 μM), and atorvastatin (1 μM) and the results showed that autophagic pathway was activated with increased the protein levels of LC3-II at 9 h and decreased the protein levels of p62 at 18 h after the treatment (Fig. 1D–F). Additionally, acridine orange staining showed that simvastatin increased autolysosomal activity in a time-dependent manner, as evidenced by a significant increase in intracellular levels of acidic vacuoles as early as 3 h, with a peak at 9 h within 18 h of treatment (Fig. 1G and H). Moreover, immunocytochemistry showed that simvastatin stimulated the formation of autophagosomes, as evidenced by the increased levels of LC3 puncta (Fig. 1I and J). To address the involvement of autophagy in simvastatin-induced NO production, HMECs were transfected with ATG7 siRNA to interfere with autophagosome formation. Results showed that simvastatin-induced activation of autophagic pathway and NO production were abrogated by pretreating with ATG7 siRNA (Fig. 2A–E). HMECs

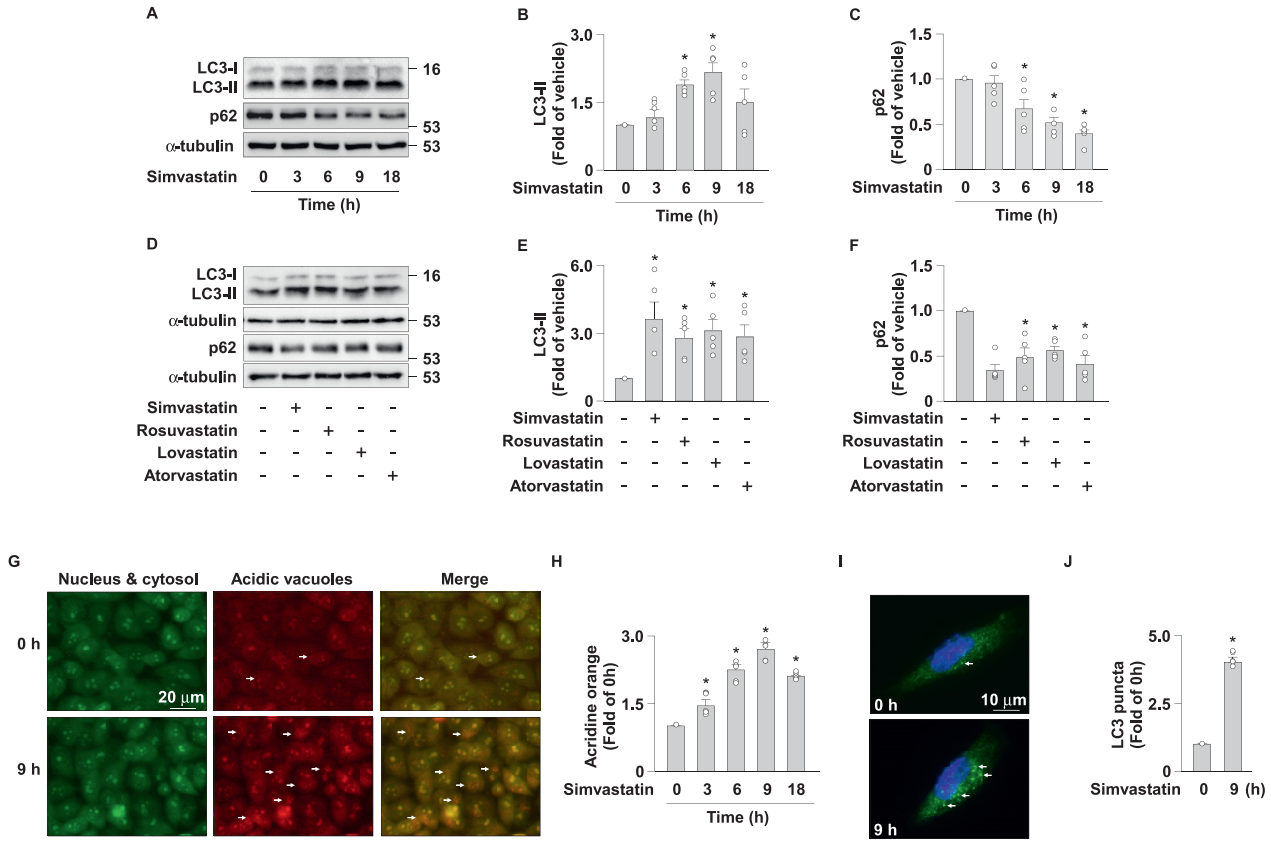


*Fig. 1. Simvastatin induces autophagy in HMECs. (A–F) HMECs were treated with simvastatin (1 μM) or various statins including rosuvastatin (1 μM), lovastatin (1 μM), and atorvastatin (1 μM) for the indicated times and treatments. (A–C) The representative images and quantitative results of Western blot analysis of LC3, p62 and α-tubulin in HMECs treated with simvastatin (1 μM) in time-course manner. (D–F) The representative images and quantitative results of Western blot analysis of LC3 at 9 h and p62 at 18 h in HMECs incubated with simvastatin, rosuvastatin (1 μM), lovastatin (1 μM), and atorvastatin (1 μM). (G–J) The representative images and quantitative results of (G and H) acridine orange staining and (I and J) LC3 puncta in HMECs treated with simvastatin for the indicated times. Arrowheads indicate (G) acidic vacuoles or (I) LC3 puncta. One-way ANOVA followed by Fisher's Least Significant Difference was used to compare data from more than two groups. Data are the mean ± SEM from five independent experiments. *P < 0.05 vs. the vehicle-treated group.*

were also pretreated with CQ or BafA1, a pharmacological inhibitor of autophagy activation. As shown in Fig. 2F–I, pretreatment with CQ or BafA1 for 2 h abolished the simvastatin-elicited activation of autophagic flux (Fig. 2F–H) and NO production (Fig. 2I). These findings suggest that activation of autophagy is required for simvastatin-induced NO production in ECs.

### *3.2. Autophagy mediates simvastatin-induced proliferation, migration, and tube formation in HMECs*

We subsequently examined whether autophagy regulated the proangiogenic effect of simvastatin on ECs. Our results revealed that simvastatin-induced increase in EC proliferation, migration, and tube formation were eliminated by pretreatment with CQ or BafA1 (Fig. 3), suggesting that autophagy plays a crucial role in the statin-mediated alterations in the physiological functions of ECs.

### *3.3. Inhibition of autophagy abolishes the simvastatin-induced activation of urea cycle in HMECs*

We next examined the effect of simvastatin on *de novo* L-arginine availability by evaluating the urea cycle activity. We found that treatment with simvastatin increased the levels of urea cycle intermediates, including glutamate, acetyl-CoA, L-arginine, and urea, and decreased the levels of ornithine in a time-dependent manner (Fig. 4A–E). Additionally, knockdown of ASL expression by a specific siRNA abrogated the simvastatin-induced increase in the levels of L-

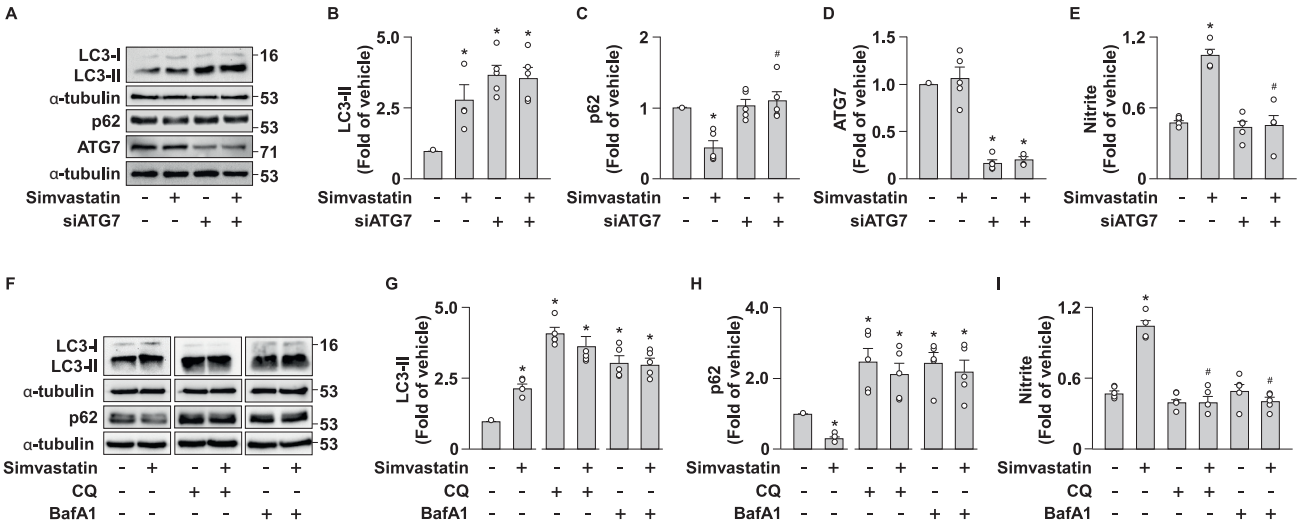


*Fig. 2. Simvastatin promotes NO bioavailability by activating autophagy in ECs. HMECs were pretreated with ATG7 siRNA (100 nM) for 24 h or pretreated with autophagy inhibitor, chloroquine (CQ, 40 μM) and bafilomycin A (BafA1, 10 nM) for 2 h, and then treated with simvastatin (1 μM) for another 9 h or 18 h. (A–C) The representative images and quantitative results of Western blot analysis of LC3 at 9 h, and p62 and ATG7 at 18 h. (D) The intracellular levels of nitrite were evaluated by Griess' assay. (F–H) The representative images and quantitative results of Western blot analysis of LC3, p62 and α-tubulin. (I) The intracellular levels of nitrite were evaluated by Griess' assay. One-way ANOVA followed by Fisher's Least Significant Difference was used to compare data from more than two groups. Data are the mean ± SEM from five independent experiments. *P < 0.05 vs. the vehicle-treated group; #P < 0.05 vs. the simvastatin-treated group.*

arginine, urea, and NO (Fig. 4F–H), suggesting that activation of the urea cycle is required for simvastatin-elicited NO production. We subsequently examined whether autophagy is involved in simvastatin-induced activation of the urea cycle. As shown in Fig. 4I-L, pretreatment with autophagy inhibitors, CQ and BafA1, prevented the simvastatin-induced increase in glutamate, acetyl-CoA, L-arginine, and urea in ECs. Moreover, pretreatment with ASL siRNA prevented simvastatin-induced proangiogenic effects (Fig. 5). These results suggest that simvastatin induces autophagy activation and provides glutamate and acetyl-CoA for the initiation of the urea cycle, leading to an

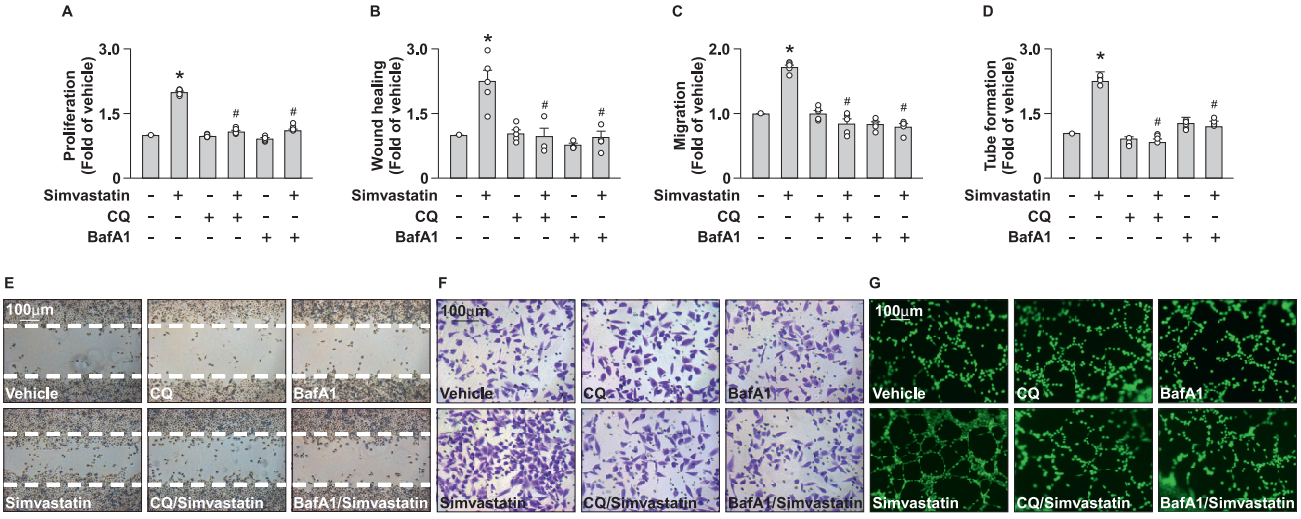


*Fig. 3. Autophagy mediates simvastatin-induced proliferation, migration, and tube formation in ECs. HMECs were pretreated with CQ (40 μM) or BafA1 (10 nM) for 2 h and then incubated with simvastatin (1 μM) for additional 18 h. (A) The EC proliferation was assessed using the MTT assay. (B–D) The EC migration and tube formation were evaluated by the wound healing assay, trans-well assay, and tube formation assay. (E–G) The representative images of (E and F) HMEC migration and (G) tube formation. One-way ANOVA followed by Fisher's Least Significant Difference was used to compare data from more than two groups. Data are the mean ± SEM from five independent experiments. *P < 0.05 vs. the vehicle-treated group; #P < 0.05 vs. the simvastatin-treated group.*

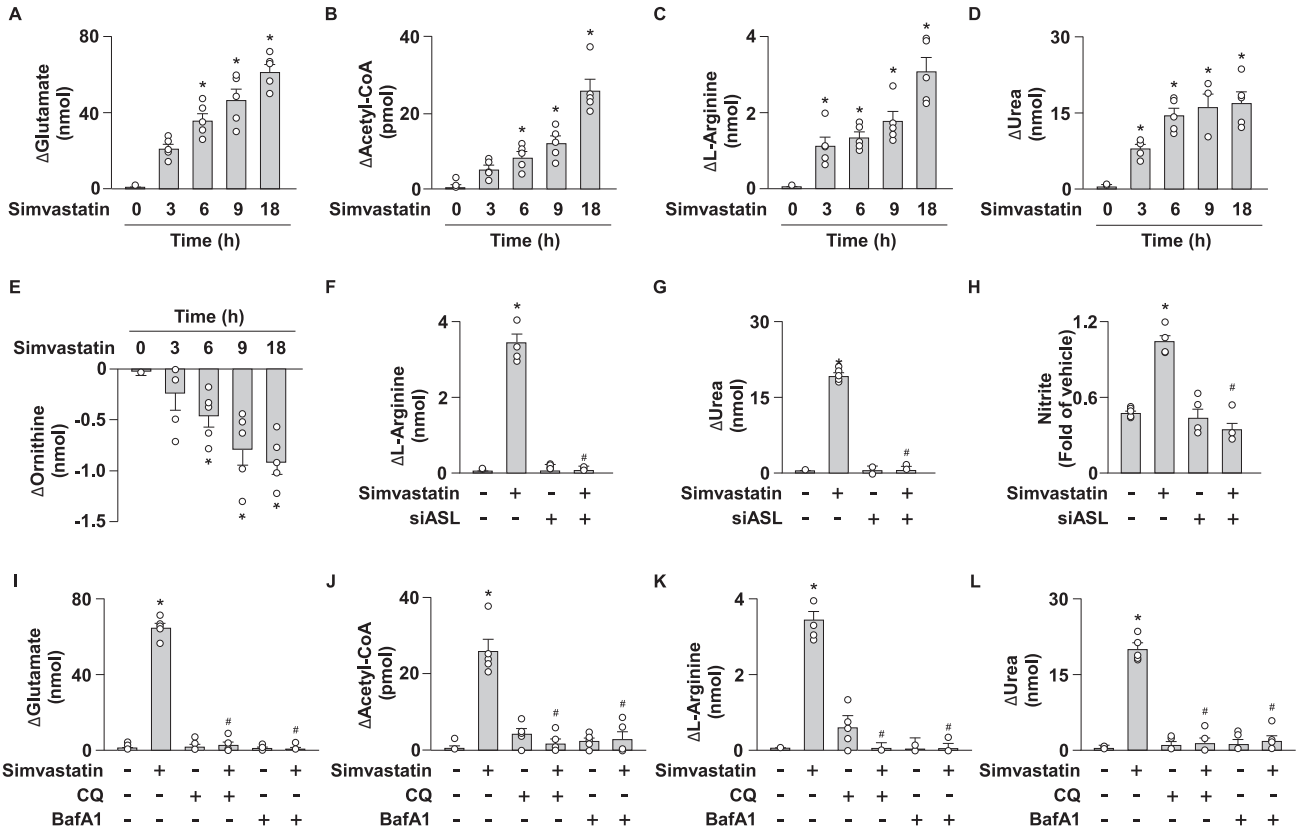


*Fig. 4. Inhibition of autophagy abolishes the simvastatin-activated urea cycle activation in ECs. (A–E) HMECs were treated with simvastatin (1 μM) for the indicated times. The changes in the levels (Δ) of (A) glutamate, (B) acetyl-CoA, (C) L-arginine, (D) urea, and (E) ornithine were assessed as compared to vehicle-treated group. (F and G) HMECs were pretreated with ASL siRNA (80 nM) for 24 h and then incubated with simvastatin (1 μM) for additional 18 h, and the changes in the levels of (F) L-arginine and (G) urea were evaluated as compared to vehicle-treated group. (H) The levels of nitrite were determined by Griess' assay. (I–L) HMECs were pretreated with CQ (40 μM) or BafA1 (10 nM) for 2 h and then incubated with simvastatin (1 μM) for another 18 h. The changes in the levels of (I) glutamate, (J) acetyl-CoA, (K) L-arginine, and (L) urea were evaluated as compared to vehicle-treated group. The value of Δ is defined by the concentration difference in each group from the group of 0 h or vehicle-treated group. One-way ANOVA followed by Fisher's Least Significant Difference was used to compare data from more than two groups. Data are the mean ± SEM from five independent experiments. *P < 0.05 vs. the vehicle-treated group; #P < 0.05 vs. the simvastatin-treated group.*

increase in *de novo* L-arginine availability, promoting NO production in ECs.

### 3.4. AMPK is required for simvastatin-mediated activation of autophagy and urea cycle in ECs

We examined the role of AMPK in simvastatin-mediated autophagy and L-arginine availability using AMPK siRNA and AMPK inhibitor, C.C. Pretreatment with AMPK siRNA or C.C. abolished simvastatin-induced activation of autophagy and the formation of LC3 puncta (Fig. 6A–I). Moreover, simvastatin-induced increase in the levels of urea, L-arginine, and NO were prevented by AMPK siRNA and AMPK inhibitor (Fig. 6J-L). These findings suggest that AMPK plays a crucial role in simvastatin-induced activation of the autophagy–urea cycle-L-arginine pathway in ECs.

### 3.5. TRPV1 is involved in simvastatin-mediated autophagy in ECs

We previously reported that TRPV1/AMPK signaling is required for simvastatin-mediated eNOS activation and NO production in ECs [9]. Thus, we investigated whether TRPV1 is involved in simvastatin-induced activation of the autophagy–urea cycle-L-arginine pathway. Pretreatment with TRPV1 antagonists, CPZ and SB366791, abrogated the simvastatin-induced activation of autophagy and the formation of LC3 puncta (Fig. 7A–E). Additionally, inhibition of TRPV1 activity prevented the simvastatin-induced increase in the levels of urea, L-arginine, and NO production (Fig. 7F–H). Collectively, these results suggest that TRPV1-AMPK signaling is crucial for simvastatin-mediated activation of the autophagy–urea cycle-L-arginine pathway and NO production in ECs (Fig. 8).

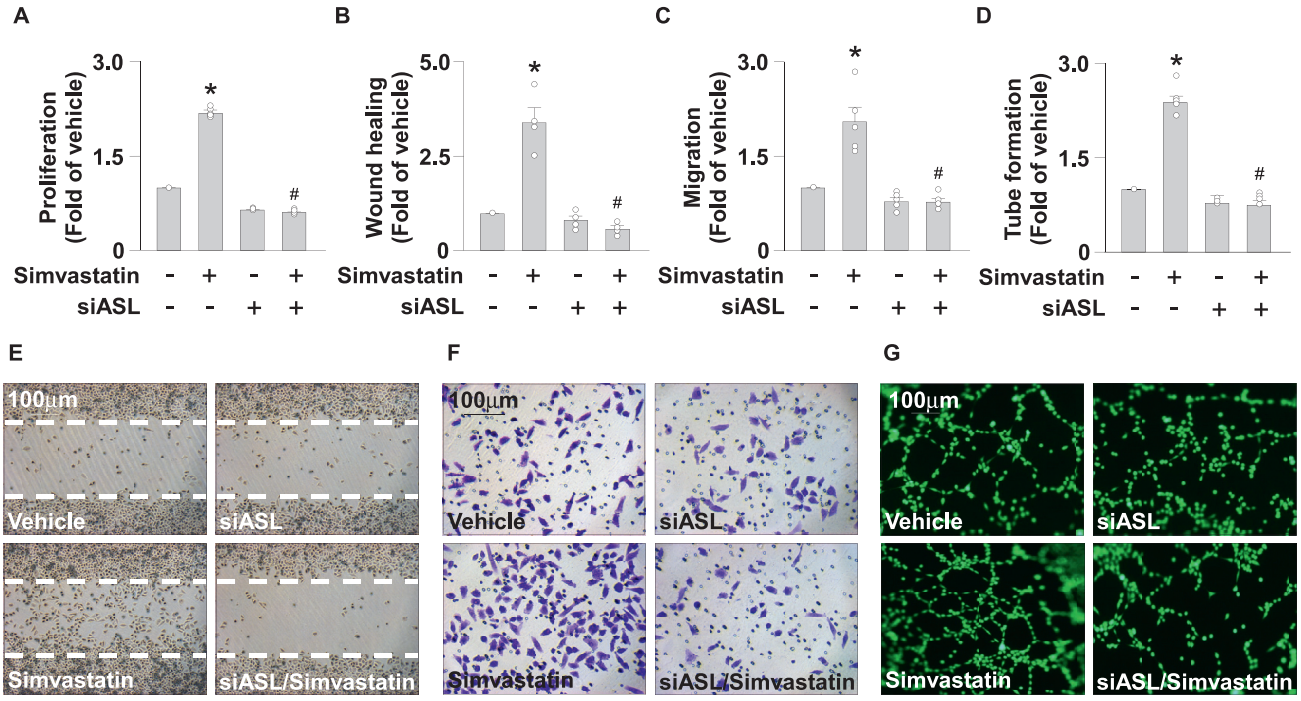


*Fig. 5. Knockdown of ASL expression prevents the simvastatin-induced increases in EC proliferation, migration and tube formation. HMECs were pretreated with ASL siRNA (80 nM) for 24 h and then treated with simvastatin (1 μM) for another 18 h. (A) EC proliferation was examined by using the MTT assay. (B–D) The quantitative results of HMEC migration and tube formation were evaluated by the wound healing assay, trans-well assay, and tube formation assay. (E–G) The representative images of HMEC migration and tube formation. One-way ANOVA followed by Fisher's Least Significant Difference was used to compare data from more than two groups. Data are the mean ± SEM from five independent experiments. *P < 0.05 vs. the vehicle-treated group; #P < 0.05 vs. the simvastatin-treated group.*

## 4. Discussion

eNOS-derived NO production in ECs is known to play an important role in the pleiotropic effects of statins in the primary prevention of cardiovascular diseases. Although the mechanisms by which statins regulate eNOS activity have been extensively studied [9,31–33], the effects of statins on the metabolism of eNOS substrate L-arginine and its regulatory mechanism remain unclear. In this study, we characterized a potential mechanism of autophagy and the urea cycle of simvastatin in the regulation of NO bioavailability and related physiological functions in ECs. In ECs, simvastatin-induced NO production was prevented by the inhibition of autophagy and the urea cycle. Mechanistically, simvastatin-activated autophagy flux to increase the levels of glutamate and acetyl-CoA, two key substrates for the initiation of the urea cycle, and resulted in an increase in L-arginine bioavailability, leading to NO production in ECs. Moreover, we previously reported that simvastatin increases EC proliferation, migration, and angiogenesis by activating the TRPV1-AMPK-eNOS signaling pathway [9]. Our current findings further showed that the TRPV1-AMPK signaling pathway is required for simvastatin-induced activation of autophagy flux and the urea cycle, and L-arginine bioavailability. Hence, simvastatin elicits TRPV1-AMPK signaling to activate eNOS and the autophagy–urea cycle pathway, which may work in concert to increase eNOS activity and L-arginine bioavailability, consequently promoting the NO production in ECs (Fig. 8). Collectively, we provide new insights into the comprehensive molecular mechanisms of simvastatin in the regulation of NO bioavailability and EC function.

Notably, Bharath et al. reported that EC autophagy is essential for the activation of eNOS and NO synthesis under shear stress stimulation [29,30], which is in line with our findings that autophagy plays a crucial role in simvastatin-induced NO production in ECs. However, the detailed molecular mechanism of autophagic flux in the biological process of NO synthesis in ECs is not fully understood. Autophagy is a key biological process for cellular homeostasis and is activated by AMPK under nutrient starvation to restore the amino acid pool by degrading and recycling proteins or cellular organelles [17–20]. Onodera and Ohsumi reported that autophagy-defective yeast failed to synthesize new proteins because of decreased intracellular levels of free amino acids [34]. Liu et al.

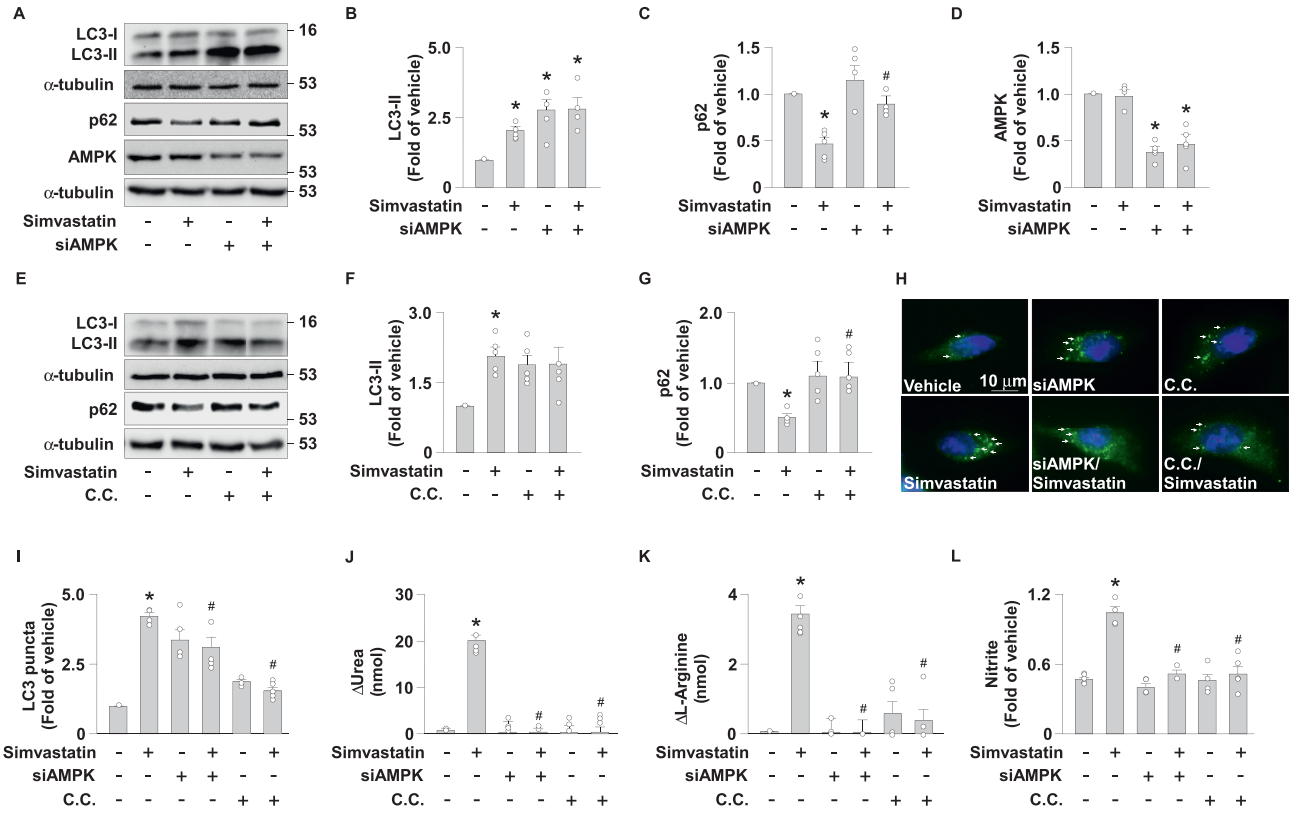


*Fig. 6. AMPK mediates simvastatin-induced activation of autophagy and urea cycle, and NO production in ECs. HMECs were pretreated with AMPK siRNA (100 nM) for 24 h or compound C (C.C., 10 μmol/L) for 2 h, then incubated with simvastatin (1 μM) for additional 9 h or 18 h. (A–D) The representative images and quantitative results of Western blot analysis of LC3 at 9 h, and p62 and AMPK at 18 h. (E–G) Western blot analysis of LC3 at 9 h and p62 at 18 h. (H and I) The representative images and quantitative results of LC3 puncta after treatment with simvastatin for 9 h. Arrowheads refer to (H) LC3 puncta. (J and K) The changes in the levels (Δ) of urea and L-arginine. The value of Δ is defined by the concentration difference in each group from vehicle-treated group. (L) The levels of nitrite in culture medium were analyzed by Griess's assay. One-way ANOVA followed by Fisher's Least Significant Difference was used to compare data from more than two groups. Data are the mean ± SEM from five independent experiments. *P < 0.05 vs. the vehicle-treated group; #P < 0.05 vs. the simvastatin-treated group.*

demonstrated that autophagy is crucial for maintaining the amino acid pool and promoting glutamate synthesis under nitrogen deprivation in yeast [35]. Moreover, Huang et al. reported that cell proliferation and vessel formation are associated with amino acids [36]. Recently, Fan et al. suggested that transcription factor EB-AMPK signaling pathway-mediated autophagy activation improves blood perfusion by increasing EC tube formation after ischemic injury [37]. In this study, we found that autophagy is required for simvastatin-induced increase in L-arginine bioavailability, NO production, and EC function. Collectively, these observations suggest that autophagy could be an important regulatory mechanism for statin-induced NO production in ECs by regulating L-arginine metabolism.

In addition to its crucial role in autophagy activation, AMPK is also involved in shear stress-induced eNOS activation and NO bioavailability [8]. Moreover, Su et al. demonstrated that simvastatin induces $Ca^{2+}$ influx through TRPV1 channels and promotes the formation of the TRPV1-Akt-calmodulin protein kinase II-AMPK-eNOS complex, which in turn induces eNOS activation, NO production, and angiogenesis in ECs [9,10]. Therefore, it was important to determine the role of TRPV1-AMPK signaling in autophagy activation and NO production. Our results confirmed that inhibition of the TRPV1-AMPK signaling pathway abolished simvastatin-induced activation of the autophagy–urea cycle pathway, L-arginine availability, and NO production. Collectively, our findings suggest that simvastatin elicits TRPV1-AMPK signaling to activate autophagy flux and leads to the production of glutamate and acetyl CoA, which promotes the L-arginine biosynthesis through the urea cycle. Here, we provide evidence supporting a novel molecular mechanism by which simvastatin regulates NO production. Nevertheless, whether this regulatory pathway contributes

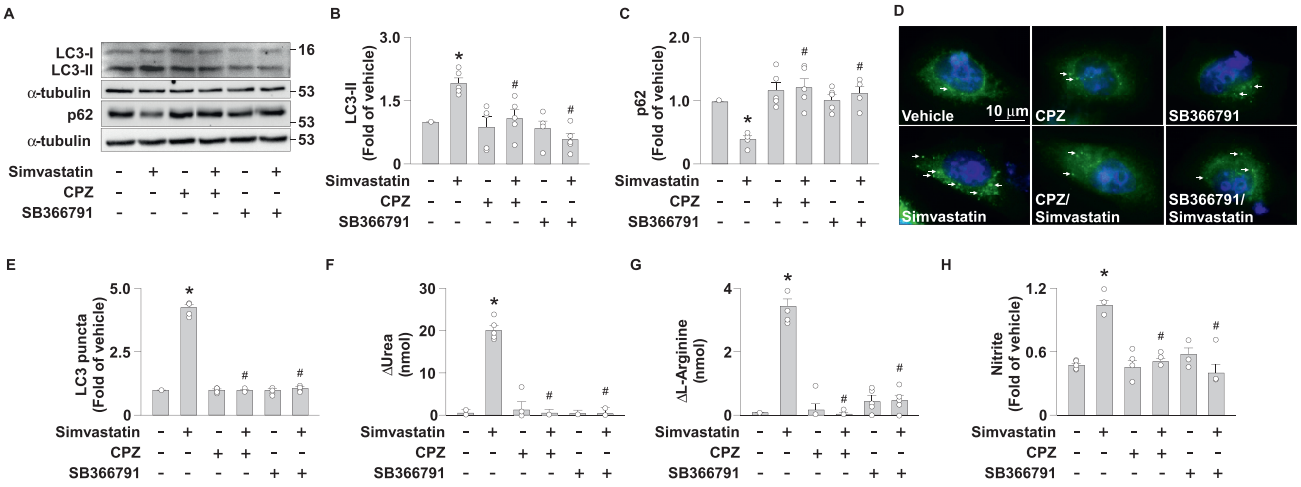


*Fig. 7. Inhibition of TRPV1 abolishes simvastatin-induced activation of autophagy and urea cycle, and NO production. HMECs were pretreated with TRPV1 pharmacological antagonist, capsazepine (CPZ, 10 μM) or SB-366791 (10 μM) for 2 h and then incubated with simvastatin (1 μM) for another 9 h or 18h. (A–C) Western blot analysis of LC3 at 9 h and p62 at 18 h. (D and E) The representative images and quantitative results of LC3 puncta after treatment with simvastatin for 9 h. Arrowheads refer to (D) LC3 puncta. (F and G) The changes in the levels (Δ) of urea and L-arginine were determined as compared with vehicle-treated group. The value of Δ is defined by the concentration difference in each group from vehicle-treated group. (H) The levels of nitrite in culture medium were assessed by Griess' assay. One-way ANOVA followed by Fisher's Least Significant Difference was used to compare data from more than two groups. Data are the mean ± SEM from five independent experiments. *P < 0.05 vs. the vehicle-treated group; #P < 0.05 vs. the simvastatin-treated group.*

to NO bioavailability induced by other stimuli requires further investigation.

L-arginine, an essential amino acid, serves as a precursor for the synthesis of NO, urea, and protein, and plays a crucial role in cell metabolism and human health [13,38]. In addition to the regulation by eNOS enzymatic activity, NO biosynthesis is tightly controlled by the levels of L-arginine, which is converted from citrulline through the activity of argininosuccinate synthase and ASL, two key enzymes of the urea cycle [39–42]. The urea cycle is responsible for detoxification of ammonia and *de novo* L-arginine synthesis [14,43]. Defective functions of urea cycle enzymes, called urea cycle disorders, can cause hyperammonemia and impairment in NO biosynthesis due to the decreased L-arginine levels, suggesting an interplay between the urea cycle and NO bioavailability [44].

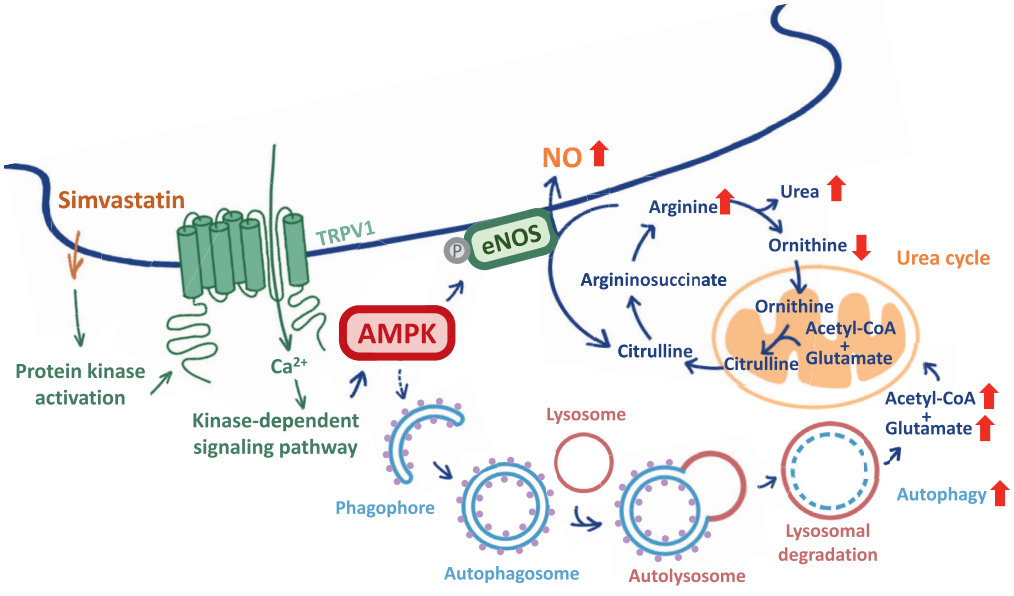


*Fig. 8. Schematic illustration of the proposed molecular mechanisms by which simvastatin elicits TRPV1-AMPK signaling and in turn activates the autophagy–urea cycle pathway to induce an increase in L-arginine bioavailability, leading to NO production in ECs.*

To the best of our knowledge, the detailed molecular mechanism of the urea cycle and NO synthesis is not fully understood. To this notion, our findings demonstrate that the activity of the urea cycle is increased by simvastatin treatment, increasing the levels of L-arginine and urea. Our results agree with those of Trupp et al. who found that administration of simvastatin altered the metabolic signature in the plasma of patients, including increased levels of citrulline and ornithine [45]. However, we observed that simvastatin treatment decreased the ornithine levels; this discrepancy could be due to the high consumption of ornithine to overcome the increased activity of the urea cycle by simvastatin in a cell culture system.

Interestingly, several lines of evidence suggest that extracellular L-arginine can be transported into cells via CAT-1 for NO production in ECs under normal physiological condition [46–49]. However, effects of simvastatin on the protein expression of CAT-1 and the subsequent transportation of L-arginine to ECs remain elusive. To this end, we examined the effect of simvastatin on the protein expression of CAT-1 and found that simvastatin did not alter the protein expression of CAT-1 in ECs (Fig. S3), consistent with previous findings that exposure to laminar shear stress did not change mRNA and protein levels of CAT-1 in ECs [50]. Taken together, our findings suggest that simvastatin increases the levels of L-arginine in ECs to promote NO biosynthesis, which may be attributed to the urea cycle activation. However, we cannot rule out the possibility of CAT-1 activity-mediated L-arginine uptake from extracellular fluid, as suggested by previous studies using other experimental conditions [46–49]. Regardless of these possibilities, our results indicate the importance of L-arginine derived from the urea cycle in simvastatin-induced NO production.

The physiological function of L-arginine in human health is mainly determined by NO, which is the major end product of L-arginine metabolism [51]. Several lines of evidence showed that NO increases glucose uptake and fatty acid oxidation in various tissues [51,52], suggesting the potential role of L-arginine in the regulation of carbohydrate and lipid metabolism, as well as the development of related metabolic diseases. Growing clinical observations indicated that *de novo* arginine synthesis is decreased in individuals with obesity [53–58]. Supplementation with L-arginine improves insulin sensitivity and endothelial function, and thus ameliorates metabolic syndrome in patients with obesity and type 2 diabetes (T2D) [51,54–58]. Here, we provide the evidence that simvastatin increases the intracellular levels of L-arginine in ECs via autophagy–urea cycle pathway, suggesting the key role of L-arginine metabolism in the protective effect of statins against cardiovascular diseases and metabolic syndrome. Notably, several clinical studies by meta-analysis demonstrated that long-term statin therapy is associated with impaired carbohydrate metabolism and an increased risk of developing T2D, particularly in patients with metabolic syndrome [59–61]. Mechanistically, *in vitro* and *in vivo* studies showed that treatment with statins downregulate the expression and translocation of glucose transporter 4 in adipocytes and skeletal muscle myotubes, and thus impair the activation of insulin signaling pathway, which may be the key molecular mechanism underlying the unfavored effect of statins on glucose metabolism and the development of T2D [62–64]. Accordingly, the effect of statins on L-arginine metabolism and glucose homeostasis seems to be controversial. To this notion, the benefit-to-harm balance of long-term statin therapy on patients with metabolic syndrome warrants further investigations.

Importantly, TRPV1 is non-cation channel with a preference for $Ca^{2+}$ that is "directly" activated by capsaicin and noxious temperature (>43 °C). Moreover, TRPV1 activity can be "indirectly" regulated by protein kinases activated by inflammatory mediators or arachidonic acid metabolites [65]. Protein kinases A (PKA) induces the phosphorylation of TRPV1 channels and increases its activity; in contrast, PKC causes the dephosphorylation of TRPV1 channels and decreases its activity. This notion was supported by our previous findings that simvastatin activates TRPV1 and increases the intracellular levels of $Ca^{2+}$, which leads to phosphorylation of AMPK, increases in the formation of TRPV1-AMPK-eNOS complex, eNOS phosphorylation and activation, NO production and, ultimately, angiogenesis in ECs [9]. Although we cannot rule out the possibility that statins can "directly" activate TRPV1 channels; we believe that the protein kinase-dependent activation is involved in the statin-mediated regulation of TRPV1 activity. Regarding to the role of TRPV1 in inhibition of HMG-CoA reductase by statins, we performed additional experiments to examine the role of TRPV1 channels in the cholesterol-lowering effect of simvastatin by assessing the protein levels of SREBP2, the transcription factor for *de novo* cholesterol synthesis, and LDLR, the receptor for LDL internalization in ECs. Pretreatment with TRPV1 inhibitors, CPZ or SB366791 did not alter simvastatin-induced increase in protein levels of SREBP2 and LDLR (Fig. S5), indicating the inhibitory effect of simvastatin on HMG-CoA reductase was independent from TRPV1 activation. These findings were consistent with the previous findings that the

pleiotropic effects of statins are independent of LDL-cholesterol lowering effect [66,67]. Collectively, these findings suggest that in addition to their lipid-lowering effect, statins may activate TRPV1/$Ca^{2+}$ signaling and increase the interaction of TRPV1, AMPK and eNOS, and lead to NO bioavailability. These two events may work in concert to reduce cardiovascular risk.

However, our study contains several limitations. First, we used only *in vitro* model to investigate the role of the autophagy–urea cycle-L-arginine pathway in statin-induced NO production and related EC functions. Our *in vitro* results from ECs cannot be fully extrapolated to *in vivo* conditions, and hence, additional studies are warranted to define the specific role of the autophagy–urea cycle-L-arginine pathway in statin-mediated EC protection. Second, using autophagy-related gene deficiency *in vivo* models of cardiovascular diseases will be helpful in clarifying the role of autophagy-mediated NO production in the vascular protection of statins. Third, we did not conduct clinical trials to support our observations from *in vitro* studies. Further *in vivo* studies or clinical trials describing the implications of the autophagy–urea cycle pathway in statin-conferred vascular protection against EC dysfunction and atherosclerosis are warranted.

In conclusion, our results provide new evidence for a better understanding of the vascular protection of statins on NO production in ECs by stimulating TRPV1-AMPK signaling to activate the autophagy–urea cycle-L-arginine pathway and eNOS activation. These two key events work in concert to promote the NO production. Further, we provide new insights into the role and molecular mechanism of autophagy in the regulation of NO bioavailability, which broadens the impact of autophagy in the regulation of vascular physiology and highlights its therapeutic potential in the treatment of cardiovascular diseases.

## Author contributions

Conceptualization: WH Chen, TS Lee; methodology: WH Chen, BC Guo, CH Chen, MC Hsu; formal analysis: WH Chen, BC Guo; investigation: WH Chen, BC Guo, CH Chen, MC Hsu; data curation: WH Chen, BC Guo, TS Lee; writing—original draft preparation: WH Chen, TS Lee; supervision: TS Lee; funding acquisition: TS Lee. All authors have read and approved the published version of the manuscript.

## Data availability

Data supporting the findings of this study are available from the corresponding author upon reasonable request.

### Conflicts of interest

The authors declare no conflict of interest.

## Acknowledgements

This study was supported by grants from the National Science and Technology Council, Taiwan (108-2320-B-002-032-MY3, 108-2811-B-002-542, 109-2811-B-002-566, 110-2811-B-002-534, 111-2320-B-002-016-MY3, 111-2314-B-002-071 and 111-2811-B-002-093) and Collaborative Research Projects of National Taiwan University College of Medicine, National Taiwan University Hospital and Min-Sheng General Hospital (109F005-111-N). We thank the staff of the imaging core at the First Core Labs, National Taiwan University College of Medicine, for technical assistance.

## Appendix.

*Fig. S1–5 (Results).*

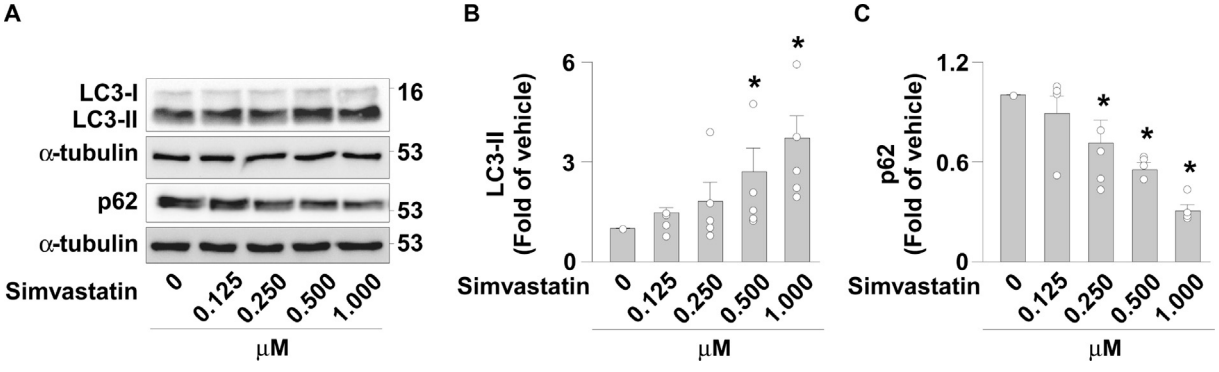


*Fig. S1. Simvastatin activates autophagy in a concentration-dependent manner. HMECs were treated with simvastatin for the indicated concentration for 9 h or 18 h. (A-C) The representative images and quantitative results of Western blot analysis of LC3 at 9 h and p62 at 18 h. One-way analysis of variance (ANOVA) followed by Fisher's Least Significant Difference was used to compare data from more than two groups. Data are the mean ± SEM from five independent experiments. *P < 0.05 vs. the vehicle-treated group.*

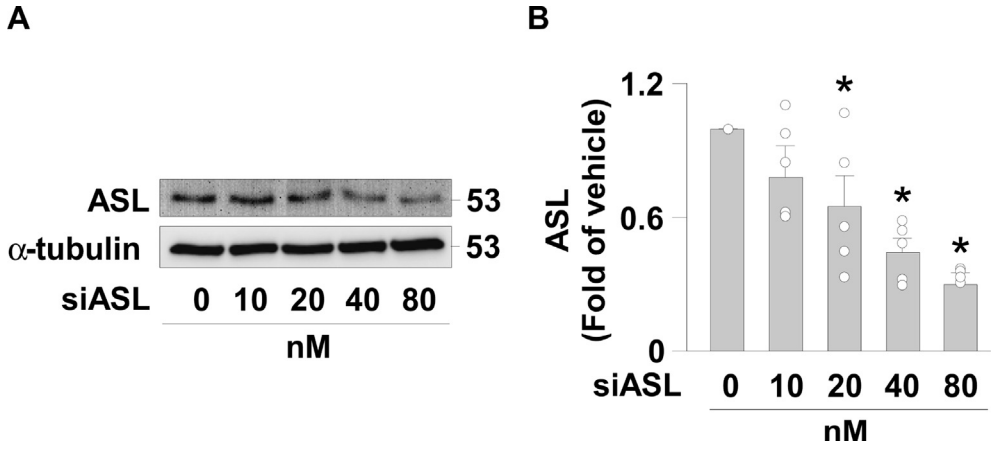


*Fig. S2. ASL expression in response to ASL siRNA. (A and B) HMECs were treated with ASL siRNA at the indicated concentrations for 24 h. Western blot analysis of ASL protein levels. One-way ANOVA followed by Fisher's Least Significant Difference was used to compare data from more than two groups. Data are the mean ± SEM from five independent experiments. *P < 0.05 vs. the vehicle-treated group.*

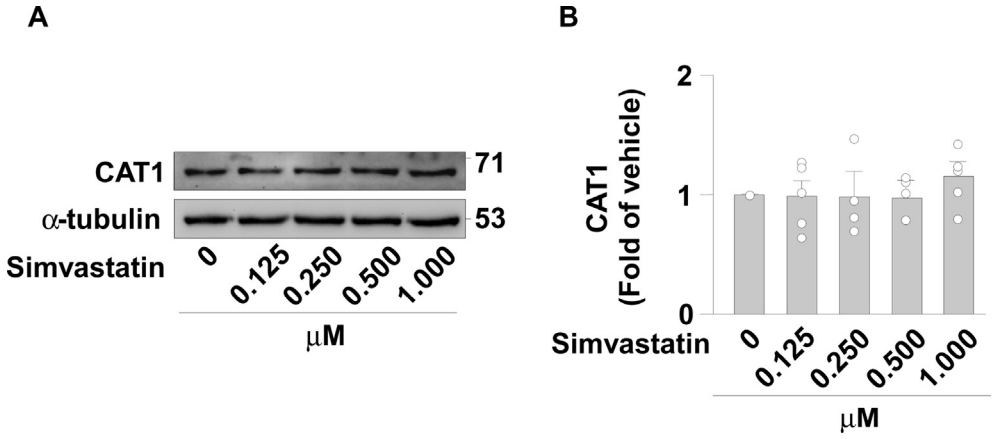


*Fig. S3. CAT-1 expression in HMECs treated with simvastatin. (A and B) HMECs were treated with simvastatin at indicated concentrations for 18 h. Western blotting analysis of protein levels of CAT-1. One-way ANOVA followed by Fisher's Least Significant Difference was used to compare data from more than two groups. Data are the mean ± SEM from five independent experiments. *P < 0.05 vs. the vehicle-treated group.*

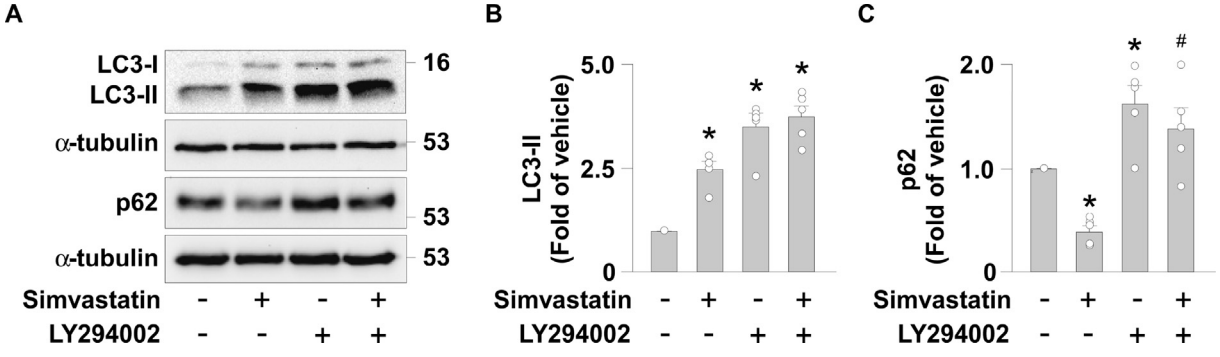


*Fig. S4. Akt mediates simvastatin-induced activation of autophagy. HMECs were pretreated with Akt inhibitor, LY294002 (10 μmol/L) for 2 h, then incubated with simvastatin (1 μM) for additional 9 h or 18 h. (A-C) The representative images and quantitative results of Western blot analysis of LC3 at 9 h, and p62 at 18 h. One-way ANOVA followed by Fisher's Least Significant Difference was used to compare data from more than two groups. Data are the mean ± SEM from five independent experiments. *P < 0.05 vs. the vehicle-treated group; #P < 0.05 vs. the simvastatin-treated group.*

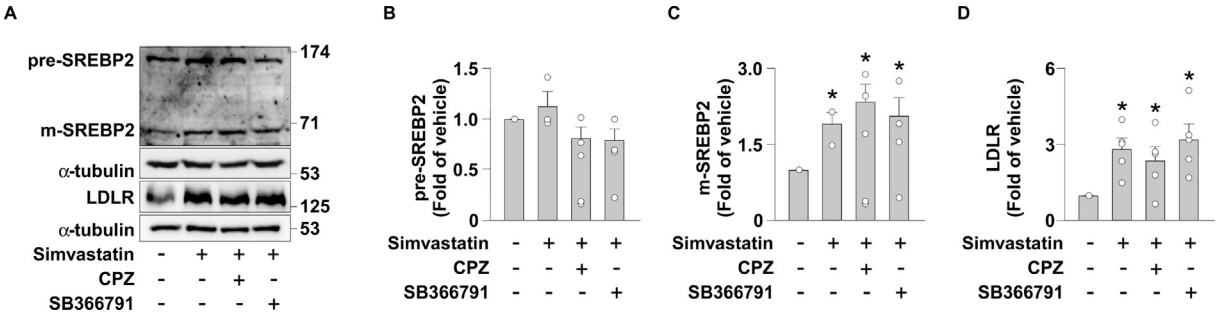


*Fig. S5. The activation of TRPV1 by simvastatin is independent from cholesterol-lowering effect. HMECs were pretreated with TRPV1 inhibitors, capsazepine (CPZ, 10 μM) or SB-366791 (10 μM) for 2 h, then incubated with simvastatin (1 μM) for additional 9 h or 18 h. (A-D) The representative images and quantitative results of Western blot analysis of pre-SREBP2 and m-SREBP2 at 9 h, and LDLR at 18 h. One-way ANOVA followed by Fisher's Least Significant Difference was used to compare data from more than two groups. Data are the mean ± SEM from five independent experiments. *P < 0.05 vs. the vehicle-treated group; #P < 0.05 vs. the simvastatin-treated group.*

## References


[1] Maron DJ, Fazio S, Linton MF. Current perspectives on statins. Circulation 2002;101:207−13.
[2] Mölgaard J, von Schenck H, Olsson AG. Effects of simvastatin on plasma lipid, lipoprotein and apolipoprotein concentrations in hypercholesterolaemia. Eur Heart J 1988;9:541−51.
[3] Heeba G, Moselhy ME, Hassan M, Khalifa M, Gryglewski R, Malinski T. Anti-atherogenic effect of statins: role of nitric oxide, peroxynitrite and haem oxygenase-1. Br J Pharmacol 2009;156:1256−66.
[4] Werner N, Nickenig G, Laufs U. Pleiotropic effects of HMG-CoA reductase inhibitors. Basic Res Cardiol 2002;97:105−16.
[5] O'Driscoll G, Green D, Taylor RR. Simvastatin, an HMG-coenzyme A reductase inhibitor, improves endothelial function within 1 month. Circulation 1997;95:1126−31.
[6] Di Napoli P, Antonio Taccardi A, Grilli A, Spina R, Felaco M, Barsotti A, et al. Simvastatin reduces reperfusion injury by modulating nitric oxide synthase expression: an ex vivo study in isolated working rat hearts. Cardiovasc Res 2001;51:283−93.
[7] Papapetropoulos A, García-Cardeña G, Madri JA, Sessa WC. Nitric oxide production contributes to the angiogenic properties of vascular endothelial growth factor in human endothelial cells. J Clin Invest 1997;100:3131−9.
[8] Zhang Y, Lee TS, Kolb EM, Sun K, Lu X, Sladek FM, et al. AMP-activated protein kinase is involved in endothelial NO synthase activation in response to shear stress. Arterioscler Thromb Vasc Biol 2006;26:1281−7.
[9] Su KH, Lin SJ, Wei J, Lee KI, Zhao JF, Shyue SK, et al. The essential role of transient receptor potential vanilloid 1 in simvastatin-induced activation of endothelial nitric oxide synthase and angiogenesis. Acta Physiol 2014;212:191−204.
[10] Kone BC. Protein-protein interactions controlling nitric oxide synthases. Acta Physiol Scand 2000;168:27−31.
[11] Vallance P, Collier J, Moncada S. Nitric oxide synthesised from L-arginine mediates endothelium dependent dilatation in human veins in vivo. Cardiovasc Res 1989;23:1053−7.
[12] Zhao Y, Vanhoutte PM, Leung SW. Vascular nitric oxide: beyond eNOS. J Pharmacol Sci 2015;129:83−94.
[13] Sakuma I, Stuehr DJ, Gross SS, Nathan C, Levi R. Identification of arginine as a precursor of endothelium-derived relaxing factor. Proc Natl Acad Sci USA 1988;85:8664−7.
[14] Luiking YC, Ten Have GA, Wolfe RR, Deutz NE. Arginine de novo and nitric oxide production in disease states. Am J Physiol Endocrinol Metab 2012;303:E1177−89.
[15] Boya P, Reggiori F, Codogno P. Emerging regulation and functions of autophagy. Nat Cell Biol 2013;15:713−20.
[16] Kim KH, Lee MS. Autophagy–a key player in cellular and body metabolism. Nat Rev Endocrinol 2014;10:322−37.
[17] Mizushima N, Klionsky DJ. Protein turnover via autophagy: implications for metabolism. Annu Rev Nutr 2007;27:19−40.
[18] Schworer CM, Shiffer KA, Mortimore GE. Quantitative relationship between autophagy and proteolysis during graded amino acid deprivation in perfused rat liver. J Biol Chem 1981;256:7652−8.
[19] Chen CH, Ho SN, Hu PA, Kou YR, Lee TS. Food preservative sorbic acid deregulates hepatic fatty acid metabolism. J Food Drug Anal 2020;28:206−16.
[20] Hsu MC, Guo BC, Chen CH, Hu PA, Lee TS. Apigenin ameliorates hepatic lipid accumulation by activating the autophagy-mitochondria pathway. J Food Drug Anal 2021;29:240−54.
[21] Kim J, Kundu M, Viollet B, Guan KL. AMPK and mTOR regulate autophagy through direct phosphorylation of Ulk1. Nat Cell Biol 2011;13:132−41.
[22] Kim J, Kim YC, Fang C, Russell RC, Kim JH, Fan W, et al. Differential regulation of distinct Vps34 complexes by AMPK in nutrient stress and autophagy. Cell 2013;152:290−303.
[23] Ezaki J, Matsumoto N, Takeda-Ezaki M, Komatsu M, Takahashi K, Hiraoka Y, et al. Liver autophagy contributes to the maintenance of blood glucose and amino acid levels. Autophagy 2011;7:727−36.
[24] Bravo-San Pedro JM, Kroemer G, Galluzzi L. Autophagy and mitophagy in cardiovascular disease. Circ Res 2017;120:1812−24.
[25] Osonoi Y, Mita T, Azuma K, Nakajima K, Masuyama A, Goto H, et al. Defective autophagy in vascular smooth muscle cells enhances cell death and atherosclerosis. Autophagy 2018;14:1991−2006.
[26] LaRocca TJ, Henson GD, Thorburn A, Sindler AL, Pierce GL, Seals DR. Translational evidence that impaired autophagy contributes to arterial ageing. J Physiol 2012;590:3305−16.
[27] Fetterman JL, Holbrook M, Flint N, Feng B, Bretón-Romero R, Linder EA, et al. Restoration of autophagy in endothelial cells from patients with diabetes mellitus improves nitric oxide signaling. Atherosclerosis 2016;247:207−17.
[28] Vion AC, Kheloufi M, Hammoutene A, Poisson J, Lasselin J, Devue C, et al. Autophagy is required for endothelial cell alignment and atheroprotection under physiological blood flow. Proc Natl Acad Sci USA 2017;114:E8675−84.
[29] Bharath LP, Mueller R, Li Y, Ruan T, Kunz D, Goodrich R, et al. Impairment of autophagy in endothelial cells prevents shear-stress-induced increases in nitric oxide bioavailability. Can J Physiol Pharmacol 2014;92:605−12.
[30] Bharath LP, Cho JM, Park SK, Ruan T, Li Y, Mueller R, et al. Endothelial cell autophagy maintains shear stress-induced nitric oxide generation via glycolysis-dependent purinergic signaling to endothelial nitric oxide synthase. Arterioscler Thromb Vasc Biol 2017;37:1646−56.

[31] Laufs U, La Fata V, Plutzky J, Liao JK. Upregulation of endothelial nitric oxide synthase by HMG CoA reductase inhibitors. Circulation 1998;97:1129−35.
[32] Laufs U, Liao JK. Post-transcriptional regulation of endothelial nitric oxide synthase mRNA stability by Rho GTPase. J Biol Chem 1998;273:24266−71.
[33] Sen-Banerjee S, Mir S, Lin Z, Hamik A, Atkins GB, Das H, et al. Kruppel-like factor 2 as a novel mediator of statin effects in endothelial cells. Circulation 2005;112:720−6.
[34] Onodera J, Ohsumi Y. Autophagy is required for maintenance of amino acid levels and protein synthesis under nitrogen starvation. J Biol Chem 2005;280:31582−6.
[35] Liu K, Sutter BM, Tu BP. Autophagy sustains glutamate and aspartate synthesis in Saccharomyces cerevisiae during nitrogen starvation. Nat Commun 2021;12:57.
[36] Huang H, Vandekeere S, Kalucka J, Bierhansl L, Zecchin A, Brüning U, et al. Role of glutamine and interlinked asparagine metabolism in vessel formation. EMBO J 2017;36: 2334−52.
[37] Fan Y, Lu H, Liang W, Garcia-Barrio MT, Guo Y, Zhang J, et al. Endothelial TFEB (Transcription Factor EB) positively regulates postischemic angiogenesis. Circ Res 2018;122: 945−57.
[38] Wu G, Meininger CJ, McNeal CJ, Bazer FW, Rhoads JM. Role of L-Arginine in nitric oxide synthesis and health in humans. Adv Exp Med Biol 2021;1332:167−87.
[39] Morris SM Jr. Regulation of enzymes of the urea cycle and arginine metabolism. Annu Rev Nutr 2002;22:87−105.
[40] Mori M, Gotoh T. Regulation of nitric oxide production by arginine metabolic enzymes. Biochem Biophys Res Commun 2000;275(3):715−9.
[41] Erez A, Nagamani SC, Shchelochkov OA, Premkumar MH, Campeau PM, Chen Y, et al. Requirement of argininosuccinate lyase for systemic nitric oxide production. Nat Med 2011;17:1619−26.
[42] Osowska S, Moinard C, Neveux N, Loï C, Cynober L. Citrulline increases arginine pools and restores nitrogen balance after massive intestinal resection. Gut 2004;53: 1781−6.
[43] Scaglia F, Brunetti-Pierri N, Kleppe S, Marini J, Carter S, Garlick P, et al. Clinical consequences of urea cycle enzyme deficiencies and potential links to arginine and nitric oxide metabolism. J Nutr 2004;134:2775S−97S.
[44] Nagasaka H, Tsukahara H, Yorifuji T, Miida T, Murayama K, Tsuruoka T, et al. Evaluation of endogenous nitric oxide synthesis in congenital urea cycle enzyme defects. Metabolism 2009;58:278−82.
[45] Trupp M, Zhu H, Wikoff WR, Baillie RA, Zeng ZB, Karp PD, et al. Metabolomics reveals amino acids contribute to variation in response to simvastatin treatment. PLoS One 2012;7:e38386.
[46] Shin S, Mohan S, Fung HL. Intracellular L-arginine concentration does not determine NO production in endothelial cells: implications on the "L-arginine paradox". Biochem Biophys Res Commun 2011;414:660−3.
[47] Simmons WW, Closs EI, Cunningham JM, Smith TW, Kelly RA. Cytokines and insulin induce cationic amino acid transporter (CAT) expression in cardiac myocytes. Regulation of L-arginine transport and no production by CAT-1, CAT-2A, and CAT-2B. J Biol Chem 1996;271:11694−702.
[48] Stevens BR, Kakuda DK, Yu K, Waters M, Vo CB, Raizada MK. Induced nitric oxide synthesis is dependent on induced alternatively spliced CAT-2 encoding L-arginine transport in brain astrocytes. J Biol Chem 1996;271: 24017−22.
[49] Kakuda DK, Sweet MJ, Mac Leod CL, Hume DA, Markovich D. CAT2-mediated L-arginine transport and nitric oxide production in activated macrophages. Biochem J 1999;340:549−53.
[50] Mun GI, Kim IS, Lee BH, Boo YC. Endothelial argininosuccinate synthetase 1 regulates nitric oxide production and monocyte adhesion under static and laminar shear stress conditions. J Biol Chem 2011;286:2536−42.
[51] Szlas A, Kurek JM, Krejpcio Z. The potential of L-arginine in prevention and treatment of disturbed carbohydrate and lipid metabolism-a review. Nutrients 2022;14:961.
[52] Jobgen WS, Fried SK, Fu WJ, Meininger CJ, Wu G. Regulatory role for the arginine-nitric oxide pathway in metabolism of energy substrates. J Nutr Biochem 2006;17:571−88.
[53] Wierzchowska-McNew RA, Engelen MPKJ, Thaden JJ, Ten Have GAM, Deutz NEP. Obesity- and sex-related metabolism of arginine and nitric oxide in adults. Am J Clin Nutr 2022;116:1610−20.
[54] Hu S, Han M, Rezaei A, Li D, Wu G, Ma X. L-arginine modulates glucose and lipid metabolism in obesity and diabetes. Curr Protein Pept Sci 2017;18:599−608.
[55] Mousavi SM, Milajerdi A, Fatahi S, Rahmani J, Zarezadeh M, Ghaedi E, et al. The effect of L-arginine supplementation on obesity-related indices: a systematic review and meta-analysis of randomized clinical trials. Int J Vitam Nutr Res 2021; 91:164−74.
[56] Wascher TC, Graier WF, Dittrich P, Hussain MA, Bahadori B, Wallner S, et al. Effects of low-dose L-arginine on insulin-mediated vasodilatation and insulin sensitivity. Eur J Clin Invest 1997;27:690−5.
[57] Bogdanski P, Sulibursk a J, Grabanska K, Musialik K, Cieslewicz A, Skoluda A, et al. Effect of 3-month L-arginine supplementation on insulin resistance and tumor necrosis factor activity in patients with visceral obesity. Eur Rev Med Pharmacol Sci 2012;16:816−23.
[58] Huynh NT, Tayek JA. Oral arginine reduces systemic blood pressure in type 2 diabetes: its potential role in nitric oxide generation. J Am Coll Nutr 2002;21:422−7.
[59] Sattar N, Preiss D, Murray HM, Welsh P, Buckley BM, de Craen AJ, et al. Statins and risk of incident diabetes: a collaborative meta-analysis of randomised statin trials. Lancet 2010;375:735−42.
[60] Crandall JP, Mather K, Rajpathak SN, Goldberg RB, Watson K, Foo S, et al. Statin use and risk of developing diabetes: results from the Diabetes Prevention Program. BMJ Open Diabetes Res Care 2017;5:e000438.
[61] Navarese EP, Buffon A, Andreotti F, Kozinski M, Welton N, Fabiszak T, et al. Meta-analysis of impact of different types and doses of statins on new-onset diabetes mellitus. Am J Cardiol 2013;111:1123−30.
[62] Nakata M, Nagasaka S, Kusaka I, Matsuoka H, Ishibashi S, Yada T. Effects of statins on the adipocyte maturation and expression of glucose transporter 4 (SLC2A4): implications in glycaemic control. Diabetologia 2006;49:1881−92.
[63] Li W, Liang X, Zeng Z, Yu K, Zhan S, Su Q, et al. Simvastatin inhibits glucose uptake activity and GLUT4 translocation through suppression of the IR/IRS-1/Akt signaling in C2C12 myotubes. Biomed Pharmacother 2016;83:194−200.
[64] Yaluri N, Modi S, Kokkola T. Simvastatin induces insulin resistance in L6 skeletal muscle myotubes by suppressing insulin signaling, GLUT4 expression and GSK-3β phosphorylation. Biochem Biophys Res Commun 2016;480: 194−200.
[65] Szallasi A, Cortright DN, Blum CA, Eid SR. The vanilloid receptor TRPV1: 10 years from channel cloning to antagonist proof-of-concept. Nat Rev Drug Discov 2007;6:357−72.
[66] Miida T, Hirayama S, Nakamura Y. Cholesterol-independent effects of statins and new therapeutic targets: ischemic stroke and dementia. J Atheroscler Thromb 2004;11:253−64.
[67] Marzilli M. Pleiotropic effects of statins: evidence for benefits beyond LDL-cholesterol lowering. Am J Cardiovasc Drugs 2010;10(Suppl 1):3−9.